

FUSED ESTIMATION OF SPARSE CONNECTIVITY PATTERNS FROM REST FMRI

Pascal Zille¹ Vince D. Calhoun^{2,4} Julia M. Stephen² Tony W. Wilson³ Yu-Ping Wang^{1,*}

¹ Biomedical Engineering Department, Tulane University.

²The Mind Research Network.

³Department of Neurological Sciences, University of Nebraska Medical Center.

⁴Department of Electrical and Computer Engineering, The University of New Mexico

ABSTRACT

Functional magnetic resonance imaging (fMRI) is a powerful tool to analyze brain development and neuronal activity. Identifying discriminative brain regions between various groups within a population has generated great interest in recent years. In this work, we consider the problem of estimating multiple sparse, co-activated brain regions from fMRI observations belonging to different classes. More precisely, we propose a method to analyze functional connectivity differences between children and young adults. Often, analysis is conducted on each class separately. Here, we propose to rely on a generalized fused Lasso penalty to extract both class-specific and shared co-expressed regions. In order to validate our method, experiments are performed on an fMRI dataset comprised of normally developing children from 8 to 21. The results demonstrate that the proposed method is able to properly extract meaningful sub-networks, which results in improved classification accuracy between the two classes.

Index Terms— Sparse Models, Joint Lasso, Classification, Brain Development.

1. INTRODUCTION

Neuroimaging is heavily used to analyze both brain function and brain structure. Over the past decade, many studies have utilized fMRI to analyze various functional activity patterns in different groups. It is often assumed that the brain operates as a set of distributed sub-networks[1] that co-activate along time. As a consequence, there is a great interest in correctly identifying these sub-networks. For example, the analysis of resting state fMRI (i.e., in the absence of an experimental task to be performed by the subject) enables one to extract the spontaneous patterns of neuronal activity when a person is at rest. Many such common patterns or co-activated entities including, e.g., the default mode network (DMN) or the sensory motor network, are now well known and identified by the research community[2]. There are many ways to extract meaningful information from fMRI blood-oxygenation-level dependent (BOLD) time series, and a compelling framework is to represent the brain as a network in which:

- Nodes are often defined from a given list of regions of interest (ROI, e.g. based on brain atlases[3], data-driven components [4]) or even down to single voxels;
- Edges are characterized by the co-activation between pairs of nodes: one quantity of interest is functional connectivity, defined as the pairwise correlation between nodes along the entire BOLD time series.

Various computational approaches have been proposed for the identification of such sub-networks. One of the most common approaches for functional connectivity analysis is probably Seed-based correlation analysis (SBA), which identifies sets of voxels that are correlated with a user-specified seed region. Independent component analysis (ICA) is an interesting data-driven tool that has been applied[5] to identify statistically independent spatial/temporal maps from BOLD time series. Non-negative Matrix Factorization (NMF) methods[6, 7] are increasingly used to extract multiple potentially overlapped brain networks by decomposing data matrices into linear combinations of non-negative basis functions. Others have been relying on partial correlation[8, 9] to define edges in the network representing the brain. More recently, Eavani et al.[1] defined quantities referred to as sparse connectivity patterns (SCP). Extracted from subjects' pairwise correlation matrices, these SCP are essentially sparse, spatially distributed and synchronous sub-networks that are supposed to represent different co-activated brain functional regions. We provide further details about their formulation and estimation in the next section. Although the same authors proposed a similar model with a discriminative flavor earlier in [10], in both works, they only extract one global set of SCP for the entire population. In this work, we extend such formulation to work with data belonging to different group/classes. This allows us to naturally extract class-specific sets of SCP. Furthermore, we propose to use a generalized fused Lasso penalty to estimate these sets of SCP by jointly using data from both classes. This leads to an increased estimation power in terms of SCP components that are common between children and young adults, which as a consequence is of great help to identify class-specific patterns within these SCP as well.

The rest of this paper is organized as follows: we present in Section 2 the concept of SCP introduced by Eavani et al.[1] and propose an extended formulation in the case of multi-class setups. Our new method is then evaluated on a real dataset (PNC[11] dataset) in Section 3, followed by some discussions and concluding remarks in Section 4.

2. IDENTIFYING SHARED NETWORKS

2.1. Presentation of the model

We start by formulating the problem of SCP identification as defined by Eavani et. al in[1]. Let us assume we have $n \in \mathbb{N}$ subjects. For each subject, a BOLD time series of n_t time points and p ROI ($n_t, p \in \mathbb{N}$) is available. Denote $C_i \in \mathbb{R}^{p \times p}$, $i = 1..n$ the correlation matrix for each subject: $C_i(p_1, p_2)$ simply is the temporal Pearson correlation value between ROI p_1 and p_2 . We can estimate $d \in \mathbb{N}$ ($d \leq p$) SCP by solving the following problem:

$$\min_{x \in \mathbb{R}^{p \times d}, \mathbf{W}} \frac{1}{2} \sum_{i=1}^n \|C_i - xW_i x^T\|_F^2 + \lambda_1 \|x\|_1 \quad (1)$$

where λ_1 is a non-negative model parameter, $\|\cdot\|_F$ denotes the Frobenius norm, $W_i \in \mathbb{R}^{d \times d}$ is a diagonal matrix, and $\mathbf{W} = \{W_1, \dots, W_n\}$. Obviously, Eq.1 boils down to a sparse population-level rank- d approximation of the set of correlation matrices over all subjects. Coefficients from W_i provide 'subject-specific' maps, while the d columns of x each define a SCP, i.e. a set of co-activated regions. Essentially, such approach reduces the high dimensionality of the correlation matrix by extracting a small set of strongly correlated components. Let us now assume our observations can be divided into K distinct classes. This can be represented with a label value $y_i \in \mathbb{Z}$, $i = 1..n$ for each subject. A direct 'supervised-flavored' extension of Eq.1 would be to solve the following problem:

$$\min_{\mathbf{x}, \mathbf{W}} \frac{1}{2} \sum_{k=1}^K \frac{1}{|\mathcal{N}_k|} \sum_{i \in \mathcal{N}_k} \|C_i - x_k W_i x_k^T\|_F^2 + \lambda_1 \sum_{k=1}^K \|x_k\|_1 \quad (2)$$

where \mathcal{N}_k is the set of observations belonging to the k -th class ($k = 1..K$), $\mathbf{x} = \{x_1, \dots, x_K\}$ and $x_k \in \mathbb{R}^{p \times d}$ is the SCP for the k -th class. Let us stress the fact that the model from Eq.2 essentially amounts to perform a separate analysis on populations from different classes. In practice, one would expect the set of SCPs x_k , $k = 1..K$ to share a certain degree of similarity with the SCP belonging to other classes. By performing separate analysis, we can not exploit these similarities. Conversely, estimating a global model for all classes might overlook some important distinctions between the classes. Inspired by the work of Danaher[12], we propose to further regularize model from Eq.2 in order to take into account shared

patterns among classes. This new model takes the following form:

$$\min_{\mathbf{x}, \mathbf{W}} \frac{1}{2} \sum_{k=1}^K \frac{1}{|\mathcal{N}_k|} \sum_{i \in \mathcal{N}_k} \|C_i - x_k W_i x_k^T\|_F^2 + \lambda_1 \sum_{k=1}^K \|x_k\|_1 + \lambda_2 \sum_{k,k'} \|x_k - x_{k'}\|_1 \quad (3)$$

where λ_2 is a non-negative model parameter. We can see that this new regularization term essentially amounts to applying the ℓ_1 penalty between corresponding elements of each pair of SCP across classes. As a result, for increasing values of λ_2 , more and more components of x_1, \dots, x_K will be identical: it encourages different classes to share SCP components. Such penalty has been applied before to joint Gaussian graphical model estimation[12] as well as cross-correlation analysis formulation for extracting imaging genomic modules [13]. A schematic diagram illustrating our approach can be seen in Figure 1. In the next section, we provide some details on how to solve Eq.3, specifically in the case where $K = 2$.

2.2. Optimization

In order to optimize the model defined in Eq.(3), we rely on the alternating direction method of multipliers[14] (ADMM). Based on variable splitting, it provides a generic and powerful framework to solve a wide variety of problems. Let us consider the following problem:

$$\begin{aligned} \min_{x,z} \quad & f(x) + g(z) \\ \text{s.t.} \quad & x - z = 0 \end{aligned} \quad (4)$$

By setting $f(x) = \sum_{k=1}^K \frac{1}{|\mathcal{N}_k|} \sum_{i \in \mathcal{N}_k} \|C_i - x_k W_i x_k^T\|_F^2$ and $g(z) = \lambda_1 \sum_{k=1}^K \|z_k\|_1 + \lambda_2 \sum_{k,k'} \|z_k - z_{k'}\|_1$, we essentially fall back into a split version of Eq.(3). It can be shown[14] that solving Eq.(4) can be done by breaking down the original optimization into several subproblems that are often much easier to solve separately. The general form of the minimization algorithm can be seen in Algorithm 1.

Algorithm 1 General ADMM minimization algorithm

- 1: Initialize $x_0, z_0, u_0 \in \mathbb{R}^p$
 - 2: Input parameter $\rho \in \mathbb{R}$
 - 3: **for** $k = 0$ to Convergence **do**
 - 4: $x_{k+1} := \operatorname{argmin}_x \left(f(x) + \frac{\rho}{2} \|x - z_k + u_k\|_2^2 \right)$
 - 5: $z_{k+1} := \operatorname{argmin}_z \left(g(z) + \frac{\rho}{2} \|z - x_k - u_k\|_2^2 \right)$
 - 6: $u_{k+1} := u_k + x_k - z_k$
 - 7: **end for**
-

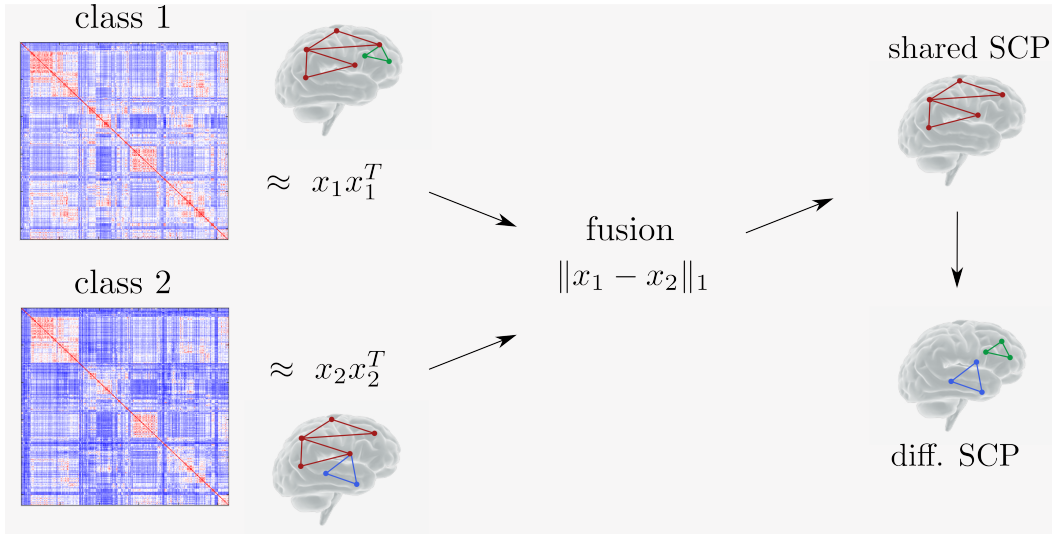


Fig. 1. Simplified illustration of the proposed method. Using correlation matrices from each classes, we extract sets of co-activated sub-networks (called SCP) represented by the components of vectors x_k , $k = 1, 2$. In this simple case, a single SCP is estimated for each class. These SCP are fused during estimation and across classes depending on the weight parameter λ_2 in Eq.3. This allows us to extract SCP components that are shared across classes (red sub-network), which in turns facilitates further identification of differential/class-specific SCP (green and blue sub-networks).

Fortunately, an efficient initialization of x_0 that proved to work well during our experiments can be obtained at fairly low cost: one just needs to perform a rank- d approximation of each $\bar{C}_k = \sum_{i \in \mathcal{N}_k} C_i$, i.e. the mean correlation matrix for each class. In our case, solving the x -update of Algorithm 1, line 4, with a few gradient estimations has proven to be efficient during our tests. Regarding the z -update of line 5, an efficient method in the case of $K = 2$ classes is detailed in [12]. In such case, a closed form solution for the minimum $z^* = (z_1^*, z_2^*)$ can be obtained in two steps. First, we calculate:

$$(z_1^*, z_2^*) = \begin{cases} (z_1 - \lambda_2/\rho, z_2 + \lambda_2/\rho) & \text{if } z_1 > z_2 + 2\lambda_2/\rho \\ (z_1 + \lambda_2/\rho, z_2 - \lambda_2/\rho) & \text{if } z_2 > z_1 + 2\lambda_2/\rho \\ (\frac{z_1+z_2}{2}, \frac{z_1+z_2}{2}) & \text{if } |z_1 - z_2| \leq 2\lambda_2/\rho \end{cases}$$

where the above operations have to be taken component wise, although the component index is omitted for the sake of simplicity. Finally, we just need to apply a soft-thresholding[15] operator with a factor of λ_1/ρ to the resulting (z_1^*, z_2^*) . In the case where more than two classes are present, more advanced and computationally expensive methods have to be used. In this work, we will restrict ourselves to only 2 classes, and refer the reader to [12] for further details.

3. EXPERIMENTS

3.1. Data acquisition and preprocessing

The Philadelphia Neurodevelopmental Cohort[11] (PNC) is a large-scale collaborative work between the Brain Behaviour

Laboratory at the University of Pennsylvania and the Children’s Hospital of Philadelphia. It is available in the dbGaP database, and contains (among other data modalities[16]) rest fMRI data for nearly 900 adolescents ages 8 to 21. Standard preprocessing steps were applied using SPM12¹, including motion correction, spatial normalization to standard MNI space and spatial smoothing with an 8mm FWHM Gaussian kernel. The influence of motion was further addressed using a regression procedure, and the functional time series were band-pass filtered using a 0.01Hz to 0.1Hz frequency range. Finally, we reduced the dimension of the data by using the 264 ROI atlas as defined by Power et al.[3]. Since we are interested in brain development with age, we select a subset of the full dataset based on age in months. More precisely, each subject whose age is over 220 months will belong to the first class (young adults cohort, age 19.54 ± 0.94 years, 87 females out of 167 subjects), while each subject whose age is under 140 months will belong to the second class (young cohort, age 10.27 ± 0.85 years, 101 females out of 165 subjects)

3.2. Joint SCP estimation

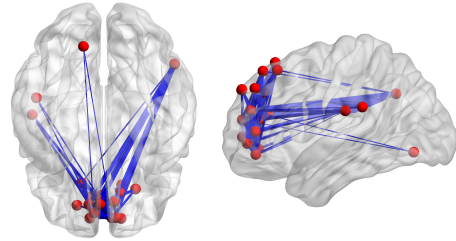
As mentioned before, we can compute a correlation matrix for each subject based on the pre-processed regional time series. We can then apply the model described in Eq.(3) to these correlation matrices. Shared components will be defined as the pairs $(i, j) \in [1..p] \times [1..d]$ such that $|\hat{x}_1(i, j) - \hat{x}_2(i, j)| > 0$,

¹<http://www.fil.ion.ucl.ac.uk/spm/>

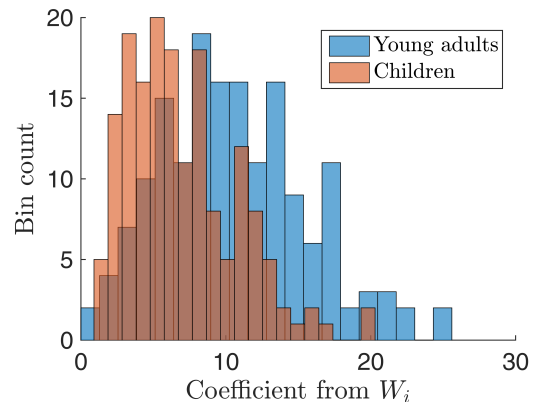
where $\hat{x}_k(i, j)$ is the i -th component of the j -th estimated SCP for the k -th class. Using that rule, we can define a shared set of SCP \hat{x}^s and differential SCP for each class $\hat{x}_k^{diff} = \hat{x}_k - \hat{x}^s$, $k = 1..2$. In order to estimate the 3 parameters (λ_1, λ_2 and d) from Eq.(3), we perform a nested grid search after having divided the original dataset into training and test subsets (80% training, 20% test). We then further divide the training set into a 5-fold sub-training/validation subset. For each fold, and for each candidate triplet (λ_1, λ_2, d), we fit the model from Eq.(3) and estimate $\hat{x}^s, \hat{x}_1^{diff}$ and \hat{x}_2^{diff} on the sub-training set. Then, we 'subtract' \hat{x}^s from each matrix $C_i, i = 1..n$, of the full training set and derive a new matrix such that $\tilde{C}_i = C_i - \hat{x}^s \tilde{W}_i (\hat{x}^s)^T$ where \tilde{W}_i is a diagonal matrix solution of $\text{argmin}_{W_i \in \mathbb{R}^{d \times d}} \|C_i - \hat{x}^s W_i (\hat{x}^s)^T\|_F^2$. The lower triangular part of each \tilde{C}_i is then used as a feature and passed to a linear SVM classifier on the validation set. The triplet (λ_1, λ_2 and d) providing the lowest classification over the 5-fold cross-validation (on the training set only) is then retained. The final accuracy of the method is then measured on the original test set. This whole procedure is repeated 10 times where each time training and test sets are chosen at random. Detailed classification results can be seen in Table 1 for the following methods: the proposed fused model from Eq.3, the separate analysis from Eq.2, and the simplest model where the lower triangular part of each of the 'raw' correlation matrices $C_i, i = 1..n$ is used as feature (hence no SCP are estimated in this case). We can observe that the fused model provides the highest accuracy as well as the highest area under the ROC Curve (AUC). The most differential SCP in our test proved to be the second differential SCP of class 1 (young adults). Each SCP's degree of 'differentiality' can be measured using a t-test between the coefficients from the weight matrix W_i corresponding to that SCP between the two classes. It is represented in Fig.2(a), where we can observe that it consists of a connectivity pattern between the frontal lobe, the right inferior parietal lobule, left supramarginal gyrus and the left superior temporal gyrus. Histograms of associated coefficients for each class are displayed in Fig.2(b), where we can see that on average young adults have a stronger expression of that particular SCP than children.

Method	Accuracy (%)	A.U.C
Fused (Eq.3)	0.92 ± 0.03	0.96 ± 0.02
Separate (Eq.2)	0.90 ± 0.02	0.95 ± 0.02
Raw Matrix	0.86 ± 0.05	0.90 ± 0.03

Table 1. Classification accuracy (%) and A.U.C values for 3 different methods, using a SVM classifier. The proposed methods produces the highest accuracy.



(a) SCP visualisation (axial and sagittal view)



(b) SCP weight for adults/children

Fig. 2. (a) Visualization of the most discriminative SCP using BrainNet Viewer Package. As can be seen in (b) this SCP is associated with much stronger reconstructive coefficients in adults than in children (p-value = $1.22e^{-12}$, t-value = 7.26).

4. DISCUSSION

This paper presented a method to extract sparse co-activated sub-networks from fMRI images. A fused penalty enforces the assumption that different groups will share some identical features. Results on real data demonstrate the discriminative power of the method compared to separate analysis of each class in the context of a brain development study between young adults and children. In particular, we found an increased connectivity between the frontal lobe, the right inferior parietal lobule, left supramarginal gyrus and the left superior temporal gyrus in young adults compared to young children. Future work will include further method validation on synthetic datasets as well as comparison with other joint penalties (e.g. group-based penalties).

5. REFERENCES

- [1] Harini Eavani, Theodore D Satterthwaite, Roman Filipovich, Raquel E Gur, Ruben C Gur, and Christos Davatzikos, "Identifying sparse connectivity patterns in the brain using resting-state fmri," *Neuroimage*, vol. 105, pp. 286–299, 2015.
- [2] Luca M De, CF Beckmann, Stefano N De, PM Matthews, and SM Smith, "fmri resting state networks define distinct modes of long-distance interactions in the human brain," *Neuroimage*, vol. 29, pp. 1359–1367, 2006.
- [3] Jonathan D Power, Alexander L Cohen, Steven M Nelson, Gagan S Wig, Kelly Anne Barnes, Jessica A Church, Alecia C Vogel, Timothy O Laumann, Fran M Miezin, Bradley L Schlaggar, et al., "Functional network organization of the human brain," *Neuron*, vol. 72, no. 4, pp. 665–678, 2011.
- [4] Elena A Allen, Erik B Erhardt, Eswar Damaraju, William Gruner, Judith M Segall, Rogers F Silva, Martin Havlicek, Srinivas Rachakonda, Jill Fries, Ravi Kalyanam, et al., "A baseline for the multivariate comparison of resting-state networks," *Frontiers in systems neuroscience*, vol. 5, pp. 2, 2011.
- [5] Vince D. Calhoun, Jingyu Liu, and Tulay Adali, "A review of group ica for fmri data and ica for joint inference of imaging, genetic, and erp data," *NeuroImage*, vol. 45, no. 1, Supplement 1, pp. S163 – S172, 2009, *Mathematics in Brain Imaging*.
- [6] Ariana Anderson, Pamela K Douglas, Wesley T Kerr, Virginia S Haynes, Alan L Yuille, Jianwen Xie, Ying Nian Wu, Jesse A Brown, and Mark S Cohen, "Non-negative matrix factorization of multimodal mri, fmri and phenotypic data reveals differential changes in default mode subnetworks in adhd," *NeuroImage*, vol. 102, pp. 207–219, 2014.
- [7] Daniel D Lee and H Sebastian Seung, "Algorithms for non-negative matrix factorization," in *Advances in neural information processing systems*, 2001, pp. 556–562.
- [8] Stephen M Smith, Karla L Miller, Gholamreza Salimi-Khorshidi, Matthew Webster, Christian F Beckmann, Thomas E Nichols, Joseph D Ramsey, and Mark W Woolrich, "Network modelling methods for fmri," *Neuroimage*, vol. 54, no. 2, pp. 875–891, 2011.
- [9] Yikai Wang, Jian Kang, Phebe B Kemmer, and Ying Guo, "An efficient and reliable statistical method for estimating functional connectivity in large scale brain networks using partial correlation," *Frontiers in neuroscience*, vol. 10, 2016.
- [10] Harini Eavani, Theodore D. Satterthwaite, Raquel E. Gur, Ruben C. Gur, and Christos Davatzikos, *Discriminative Sparse Connectivity Patterns for Classification of fMRI Data*, pp. 193–200, Springer International Publishing, 2014.
- [11] Theodore D Satterthwaite, John J Connolly, Kosha Ruparel, Monica E Calkins, Chad Jackson, Mark A Elliott, David R Roalf, Karthik Prabhakaran Ryan Hopsona, Meckenzie Behr, Haijun Qiu, et al., "The philadelphia neurodevelopmental cohort: a publicly available resource for the study of normal and abnormal brain development in youth," *Neuroimage*, vol. 124, pp. 1115–1119, 2016.
- [12] Patrick Danaher, Pei Wang, and Daniela M. Witten, "The joint graphical lasso for inverse covariance estimation across multiple classes," *Journal of the Royal Statistical Society: Series B (Statistical Methodology)*, vol. 76, no. 2, pp. 373–397, 2014.
- [13] Jian Fang, Dongdong Lin, Charles Schulz, Zongben Xu, Vince D Calhoun, and Yu-Ping Wang, "Joint sparse canonical correlation analysis for detecting differential imaging genetics modules," *Bioinformatics* (doi:10.1093/bioinformatics/btw485), 2016.
- [14] Stephen Boyd, Neal Parikh, Eric Chu, Borja Peleato, and Jonathan Eckstein, "Distributed optimization and statistical learning via the alternating direction method of multipliers," *Foundations and Trends in Machine Learning*, vol. 3, no. 1, pp. 1–122, 2011.
- [15] Jerome Friedman, Trevor Hastie, Holger Höfling, Robert Tibshirani, et al., "Pathwise coordinate optimization," *The Annals of Applied Statistics*, vol. 1, no. 2, pp. 302–332, 2007.
- [16] Theodore D Satterthwaite, Mark A Elliott, Kosha Ruparel, James Loughhead, Karthik Prabhakaran, Monica E Calkins, Ryan Hopson, Chad Jackson, Jack Keefe, Marisa Riley, et al., "Neuroimaging of the philadelphia neurodevelopmental cohort," *Neuroimage*, vol. 86, pp. 544–553, 2014.